

REVIEW

Open Access



Cardiovascular disease in women: insights from magnetic resonance imaging

Chiara Bucciarelli-Ducci¹, Ellen Ostenfeld^{2*} , Lauren A. Baldassarre³, Vanessa M. Ferreira⁴, Luba Frank⁵, Kimberly Kallianos⁶, Subha V. Raman⁷, Monvadi B. Srichai⁸, Elisa McAlindon⁹, Sophie Mavrogeni¹⁰, Ntobeko A. B. Ntusi¹¹, Jeanette Schulz-Menger¹², Anne Marie Valente¹³ and Karen G. Ordovas⁶

Abstract

The presentation and identification of cardiovascular disease in women pose unique diagnostic challenges compared to men, and underrecognized conditions in this patient population may lead to clinical mismanagement.

This article reviews the sex differences in cardiovascular disease, explores the diagnostic and prognostic role of cardiovascular magnetic resonance (CMR) in the spectrum of cardiovascular disorders in women, and proposes the added value of CMR compared to other imaging modalities. In addition, this article specifically reviews the role of CMR in cardiovascular diseases occurring more frequently or exclusively in female patients, including Takotsubo cardiomyopathy, connective tissue disorders, primary pulmonary arterial hypertension and peripartum cardiomyopathy. Gaps in knowledge and opportunities for further investigation of sex-specific cardiovascular differences by CMR are also highlighted.

Keywords: Cardiovascular magnetic resonance, Female cardiovascular disease, Ischemic heart disease, Non-ischemic cardiomyopathies, Peripartum cardiomyopathy, Chemotherapy-induced cardiomyopathy, Congenital heart disease, Turner syndrome, Connective tissue disease, Pulmonary hypertension

Background

Women are commonly underrepresented in cardiovascular research, comprising as little as 15–35% of populations in randomized clinical trials [1], and when included, are most often in the postmenopausal stage of life [2]. Even though both men and women are affected by cardiovascular disease, there are only limited numbers of sex-specific and age-balanced imaging and management guidelines for women with cardiovascular disease [2]. In the setting of growing awareness of providing personalized precision medicine, addressing sex differences in cardiovascular disease is a key goal [1].

Anatomically, women have smaller hearts even after adjustment for body size, and, as a result, have different disease phenotypes, which may influence the choice and

accuracy of diagnostic tests. Further, there are intrinsic imaging difficulties with transthoracic echocardiography in women due to reduced image quality from breast tissue attenuation and reluctance to use cardiac computed tomography (CCT) in pre-menopausal women due to breast tissue sensitivity. Cardiovascular magnetic resonance (CMR) imaging provides a comprehensive evaluation of cardiovascular disease, including assessment of myocardial structure and function, inflammation, ischemia, viability, and valvular disease, with the additional benefit of excellent reproducibility [3]. The advantage of lack of exposure to ionizing radiation is particularly beneficial in women, especially in those of childbearing and premenopausal age.

The literature on sex-specific differences in cardiovascular conditions, including sex-specific CMR reference values, is limited. The aims of this paper are to review the applications of CMR in the spectrum of cardiovascular diseases that affect women, with a particular focus on

* Correspondence: ellen.ostenfeld@med.lu.se

²Department of Clinical Sciences Lund, Clinical Physiology, Skåne University Hospital Lund, Lund University, Getingevägen 5, SE-22185 Lund, Sweden
Full list of author information is available at the end of the article



© The Author(s). 2020 **Open Access** This article is licensed under a Creative Commons Attribution 4.0 International License, which permits use, sharing, adaptation, distribution and reproduction in any medium or format, as long as you give appropriate credit to the original author(s) and the source, provide a link to the Creative Commons licence, and indicate if changes were made. The images or other third party material in this article are included in the article's Creative Commons licence, unless indicated otherwise in a credit line to the material. If material is not included in the article's Creative Commons licence and your intended use is not permitted by statutory regulation or exceeds the permitted use, you will need to obtain permission directly from the copyright holder. To view a copy of this licence, visit <http://creativecommons.org/licenses/by/4.0/>. The Creative Commons Public Domain Dedication waiver (<http://creativecommons.org/publicdomain/zero/1.0/>) applies to the data made available in this article, unless otherwise stated in a credit line to the data.

sex-related differences in conditions that occur more frequently or exclusively in women.

Comparison of normative CMR sex-specific values in healthy subjects

Table 1 lists normative values of ventricular volumes and mass in women and men.

Both absolute and indexed left ventricular (LV) and right ventricular (RV) volumes and LV mass are smaller in women compared to men. LV and RV ejection fraction (EF) are greater or equal in women compared to men [4–7, 11]. Absolute left atrial (LA) maximal volume is significantly smaller in women compared to men, however indexed LA volumes and emptying fraction are similar between sexes [4, 8, 9]. Absolute right atrial (RA) maximal volume is significantly smaller, indexed RA volume is smaller or equal, and RA emptying fraction is higher in women [4, 9, 10].

Current evidence suggests that T1 and extracellular volume (ECV) values are higher in women, especially premenopausal women, compared with men, at both 1.5 T and 3 T [12–15]. There is conflicting evidence whether CMR T2 mapping values are influenced by sex [15–18], although current studies used different T2-mapping techniques, and may be underpowered to detect sex-dependent effects. Large population based studies that include equal sex representation will allow for sex-specific reference values for T1, T2 and ECV [19].

Ischemic heart disease

Acute myocardial infarction

Acute myocardial infarction (MI) in women differs from men in presentation, underlying pathophysiology, and outcomes [20, 21]. This includes a higher mortality after acute MI in women < 50 years of age (odds ratio 1.37 for female sex) [22]. Women have a higher prevalence of non-obstructive coronary plaques [21, 23–25] and less atheroma volume than men [26], which may affect strategies for diagnosing acute coronary syndrome (ACS) in women.

CMR can characterize myocardial tissue following MI, independently of the presence of obstructive coronary lesions. Studies have shown that infarct size and myocardial salvage are smaller in women than men (myocardial salvage index: women 0.4 vs. men 0.5, $p = 0.013$), reflecting a smaller acute infarct size (women 14% of LV vs. men 22% of LV) and follow up infarct size (women 8% vs. men 13% LV) [27]. In addition, microvascular obstruction (MVO) burden has been shown to be smaller in women than in men by Canali et al. (women $1.1 \pm 1.0\%$ LV vs. men $3.4 \pm 2.2\%$ LV, $p < 0.001$) [27] and by Langerhans et al. (women $0.48 \pm 1.3\%$ LV vs. men $1.2 \pm 3.0\%$ LV, $p = 0.03$) [28].

Myocardial infarction with non-obstructed coronary arteries (MINOCA)

There is over-representation of women with MI with non-obstructed coronary arteries (MINOCA) relative to those with elevated troponin and obstructive coronary artery disease (CAD) (24–30% are women) [29, 30]. Mechanisms of MINOCA more commonly observed in women include coronary microvascular dysfunction [31–33] and coronary artery plaque erosions [34, 35]. Identification of underlying etiology of MINOCA is important for risk stratification and treatment decision-making [36, 37]. CMR is a key diagnostic imaging tool in the assessment of patients with MINOCA, providing detailed myocardial tissue characterization, location of myocardial inflammation/edema, scarring/fibrosis, and discriminating between ischemic and non-ischemic etiologies. CMR has been shown to identify the underlying etiology in up to 87% of patients with MINOCA [38]. In particular, the more common causes of MINOCA, such as myocarditis, acute MI without obstructing plaque, and Takotsubo cardiomyopathy (TCM), can be easily diagnosed with CMR. Ischemic patterns of late gadolinium enhancement (LGE) may be seen in women presenting with MINOCA [39], and abnormal perfusion on stress CMR is commonly noted, likely to be related to multiple mechanisms, including microvascular dysfunction [40]. Despite the absence of angiographically significant CAD, patients with MINOCA have worse outcomes with a 12 month all-cause mortality rate of 4.7% [29]. A recent study demonstrates that CMR can inform prognosis in MINOCA patients, independent of sex [41].

Differential diagnosis of MINOCA

Myocarditis CMR is an important tool for diagnosis of myocarditis in both sexes [42, 43]. The CMR diagnosis of myocarditis is based on the “Lake Louise criteria” of myocardial edema, hyperemia, and fibrosis (Fig. 1) [44]. In addition, parametric mapping techniques, including native T1 mapping, extracellular volumes of distribution, and T2 mapping are promising techniques and may significantly improve the diagnostic accuracy of CMR [14, 45–48].

Although there are no differences in the CMR diagnostic criteria for myocarditis in women versus men, sex-differences are noted specifically related to the subsequent risk of chronic dilated cardiomyopathy [49].

Takotsubo cardiomyopathy Takotsubo cardiomyopathy (TCM) should be considered in the differential diagnosis of MINOCA, with a prevalence of 10–27% [36, 38, 50–52]. TCM is a condition more prevalent in women and is often precipitated by an emotional or physical stress and a characteristic finding is mid-cavity

Table 1 Normative CMR values of cardiac volumes and function in women and men

	Author, year	N (women + men), age	Women	Men	Women compared to men	
Left ventricle						
LVEDV (ml)	Petersen et al., 2017 [4]	433 + 371, 45–74 years	124 (88–161)	166 (109–218)	↓	
	Maicera et al., 2006 [5]	60 + 60, 20–80 years	128 (88–168)	156 (115–198)	↓	
	Alfakih et al., 2003 [6]	30 + 30, 20–65 years	135 (96–174)	169 (102–235)	↓	
LVEDVi (ml/m ²)	Petersen et al., 2017 [4]	433 + 371, 45–74 years	74 (54–94)	85 (60–110)	↓	
	Maicera et al., 2006 [5]	60 + 60, 20–80 years	75 (57–92)	80 (63–98)	↓	
	Alfakih et al., 2003 [6]	30 + 30, 20–65 years	78 (56–99)	82 (53–112)	↓	
LVESV (ml)	Petersen et al., 2017 [4]	433 + 371, 45–74 years	49 (31–68)	69 (39–97)	↓	
	Maceira et al., 2006 [5]	60 + 60, 20–80 years	42 (23–60)	53 (30–75)	↓	
	Alfakih et al., 2003 [6]	30 + 30, 20–65 years	49	61	↓	
LVESVi (ml/m ²)	Petersen et al., 2017 [4]	433 + 371, 45–74 years	29 (19–40)	36 (21–49)	↓	
	Maceira et al., 2006 [5]	60 + 60, 20–80 years	24 (15–34)	27 (16–38)	↓	
	Petersen et al., 2017 [4]	433 + 371, 45–74 years	75 (49–100)	96 (59–132)	↓	
LVSV (ml)	Maceira et al., 2006 [5]	60 + 60, 20–80 years	86 (58–114)	104 (76–132)	↓	
	Alfakih et al., 2003 [6]	30 + 30, 20–65 years	86	108	↓	
	Petersen et al., 2017 [4]	433 + 371, 45–74 years	45 (30–59)	49 (32–67)	↓	
LVSVi (ml/m ²)	Maceira et al., 2006 [5]	60 + 60, 20–80 years	50 (38–63)	53 (41–65)	↓	
	Petersen et al., 2017 [4]	433 + 371, 45–74 years	61 (51–70)	58 (48–69)	↑	
	Maceira et al., 2006 [5]	60 + 60, 20–80 years	67 (58–76)	67 (58–75)	→	
LVEF (%)	Alfakih et al., 2003 [6]	30 + 30, 20–65 years	64 (54–74)	64 (55–73)	→	
	Petersen et al., 2017 [4]	433 + 371, 45–74 years	70 (46–93)	103 (64–141)	↓	
	Maceira et al., 2006 [5]	60 + 60, 20–80 years	108 (72–144)	146 (108–184)	↓	
LVM (g)	Alfakih et al., 2003 [6]	30 + 30, 20–65 years	90 (66–114)	133 (85–181)	↓	
	Petersen et al., 2017 [4]	433 + 371, 45–74 years	42 (29–55)	53 (35–70)	↓	
	Maceira et al., 2006 [5]	60 + 60, 20–80 years	63 (48–77)	74 (58–91)	↓	
LVMI (g/m ²)	Alfakih et al., 2003 [6]	30 + 30, 20–65 years	52 (37–67)	65 (46–83)	↓	
	Right ventricle					
	RVEDV (ml)	Petersen et al., 2017 [4]	433 + 371, 45–74 years	130 (85–168)	182 (124–258)	↓
Maceira et al., 2006 [7]		60 + 60, 20–80 years	126 (84–168)	163 (113–213)	↓	
Alfakih et al., 2003 [6]		30 + 30, 20–65 years	131 (83–178)	177 (111–243)	↓	
RVEDVi (ml/m ²)	Petersen et al., 2017 [4]	433 + 371, 45–74 years	77 (53–99)	93 (68–125)	↓	
	Maceira et al., 2006 [7]	60 + 60, 20–80 years	73 (55–92)	83 (60–106)	↓	
	Alfakih et al., 2003 [6]	30 + 30, 20–65 years	75 (48–103)	86 (58–114)	↓	
RVESV (ml)	Petersen et al., 2017 [4]	433 + 371, 45–74 years	55 (27–77)	85 (47–123)	↓	
	Maceira et al., 2006 [7]	60 + 60, 20–80 years	43 (17–69)	57 (27–86)	↓	
	Alfakih et al., 2003 [6]	30 + 30, 20–65 years	52	79	↓	
RVESVi (ml/m ²)	Petersen et al., 2017 [4]	433 + 371, 45–74 years	33 (17–46)	43 (25–63)	↓	
	Maceira et al., 2006 [7]	60 + 60, 20–80 years	25 (12–38)	29 (14–43)	↓	
	Petersen et al., 2017 [4]	433 + 371, 45–74 years	75 (48–99)	97 (68–125)	↓	
RVSV (ml)	Maceira et al., 2006 [7]	60 + 60, 20–80 years	83 (57–108)	106 (72–140)	↓	
	Alfakih et al., 2003 [6]	30 + 30, 20–65 years	78	98	↓	
	Petersen et al., 2017 [4]	433 + 371, 45–74 years	45 (30–59)	50 (34–67)	↓	
RVSVi (ml/m ²)	Maceira et al., 2006 [7]	60 + 60, 20–80 years	48 (36–60)	54 (38–70)	↓	
	Petersen et al., 2017 [4]	433 + 371, 45–74 years	58 (47–68)	54 (45–65)	↑	
	RVEF (%)					

Table 1 Normative CMR values of cardiac volumes and function in women and men (*Continued*)

	Author, year	N (women + men), age	Women	Men	Women compared to men
RVM (g)	Maceira et al., 2006 [7]	60 + 60, 20–80 years	66 (54–78)	66 (53–78)	→
	Alfakih et al., 2003 [6]	30 + 30, 20–65 years	60 (50–70)	55 (48–63)	↑
	Maceira et al., 2006 [7]	60 + 60, 20–80 years	48 (27–69)	66 (38–94)	↓
	Maceira et al., 2006 [7]	60 + 60, 20–80 years	28 (18–38)	34 (19–43)	↓
Left atrium					
LAV max (ml)	Petersen et al., 2017 [4] ^a	433 + 371, 45–74 years	62 (33–93)	71 (37–108)	↓
	Maceira et al., 2010 [8] ^c	60 + 60, 20–80 years	68 (42–95)	77 (48–107)	↓
LAVi max (ml/m ²)	Petersen et al., 2017 [4] ^a	433 + 371, 45–74 years	37 (21–55)	36 (19–55)	→
	Maceira et al., 2010 [8] ^c	60 + 60, 20–80 years	40 (27–52)	39 (26–53)	→
LA emptying fraction (%)	Petersen et al., 2017 [4] ^a	433 + 371, 45–74 years	61 (49–74)	60 (47–73)	→
	Maceira et al., 2016 [9] ^c	60 + 60, 20–80 years	60 (48–72)	58 (47–68)	↑
Right atrium					
RAV max (ml)	Petersen et al., 2017 [4] ^b	433 + 371, 45–74 years	69 (38–101)	93 (43–143)	↓
	Maceira et al., 2013 [10] ^c	60 + 60, 20–80 years	91 (58–124)	109 (64–124)	↓
RAVi max (ml/m ²)	Petersen et al., 2017 [4] ^b	433 + 371, 45–74 years	41 (23–59)	48 (22–74)	↓
	Maceira et al., 2013 [10] ^c	60 + 60, 20–80 years	53 (36–70)	55 (33–78)	→
RA emptying fraction (%)	Petersen et al., 2017 [4] ^b	433 + 371, 45–74 years	46 (31–63)	41 (23–58)	↑
	Maceira et al., 2016 [9] ^c	60 + 60, 20–80 years	58 (46–69)	54 (40–68)	↑

Data expressed as mean and in parenthesis the lower and upper reference limits (95% interval) when noted in original publication

LV Left ventricular, EDV End-diastolic volume, I Indexed to body surface area, ESV End-systolic volume, EF Ejection fraction, LVM Left ventricular mass, RV Right ventricular, LAV Left atrial volume, LA Left atrial, RAV Right atrial volume, RA Right atrial

^aVolumes from biplane, ^bVolumes from single plane 4ch view, ^cVolumes from short axis stack

to apical akinesia with sparing of the basal segments though many atypical variants have been described. While previously thought to have a favorable prognosis, recent data suggest that TCM is associated with increased arrhythmic risk and worse prognosis [53, 54]. CMR has added diagnostic value in TCM, detecting myocardial edema in regions with focal wall motion abnormalities, without the presence of myocardial scarring (Fig. 2) [55]. The typical pattern of myocardial edema is circumferential, transmural in extent, and resolves within 2–3 months along with recovery of regional wall

motion abnormality [56]. In TCM, absence of LGE rules out acute MI or myocarditis; although a subtle patchy LGE may be present, which has been attributed to the presence of edema [51, 56], sub-microscopic cell death, and transient increase in levels of extracellular matrix proteins, particularly collagen-1 [57].

Chronic coronary syndrome

The diagnosis of chronic coronary syndrome (previously referred to as stable CAD) presents several challenges in

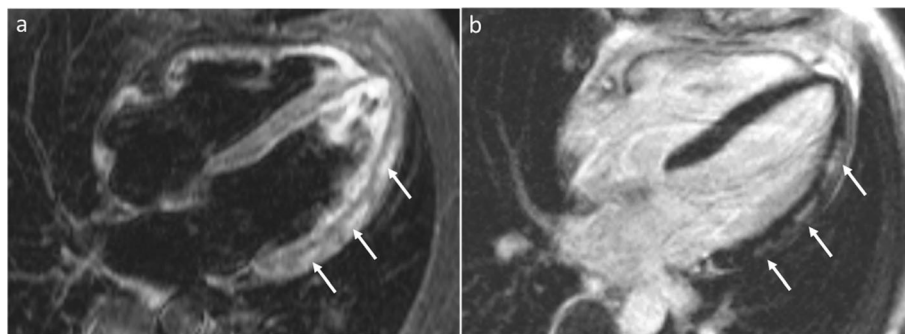


Fig. 1 Acute Myocarditis. Four chamber long-axis view T2-weighted image (a) and corresponding late gadolinium enhancement (LGE) image (b). The white arrows indicate patchy epicardial and mid-wall areas of myocardial edema a with corresponding epicardial and mid-wall late gadolinium enhancement (b)

women with suspected ischemic heart disease [73] recommends CMR in symptomatic women with intermediate risk of CAD and resting ST-segment abnormalities or inability to exercise. In premenopausal women with functional disability, stress CMR may be reasonable for the identification of obstructive CAD and estimation of prognosis [73].

Non-ischemic cardiomyopathies

Peripartum cardiomyopathy

Peripartum Cardiomyopathy (PPCM) is defined as an idiopathic cardiomyopathy manifesting as heart failure due to LV systolic dysfunction in the final weeks of pregnancy or in the first 6 months after delivery when no other cause of heart failure is found [74]. The incidence of PPCM is highly variable among geographic regions, reported as 0.1% of pregnancies, but with high morbidity and mortality rates ranging 7 to 50% [75, 76]. Cardiovascular adaptive changes occur normally during pregnancy [77], and there are published reference CMR values for cardiac indices during pregnancy and the postpartum period in healthy pregnant women aged 18 to 35 years [77]. Typically, there is an increased left ventricular end-diastolic volume (LVEDV) and increased LV mass (LVM) during pregnancy, with these values consistently underestimated by echocardiography.

While the initial imaging diagnosis of PPCM is based on echocardiography, CMR has a significant added value by accurately assessing LVEF and identifying myocardial edema and LGE [78, 79]. The mid-wall and subepicardial LGE pattern observed in PPCM can be seen in up to 40% of patients in the acute phase or in the follow up examinations. The presence and extent of LGE in PPCM has been linked to an unfavorable prognosis with slower recovery, higher risk of prolonged or permanent systolic dysfunction, and higher rate of developing heart failure exacerbation in future pregnancies (Fig. 3) [78, 79].

RV dysfunction evaluated serially by CMR has emerged as a negative prognostic indicator in patients with PPCM, as it is associated with increased dilation of both ventricles and lower LVEF, suggestive of more extensive biventricular cardiac involvement [78, 80].

Breast cancer related chemotherapy-induced cardiomyopathy

Current therapy for breast cancer with anthracyclines and trastuzumab has resulted in significantly improved survival in women; however, it is associated with increased cardiovascular events, with over 7 times increased risk of heart failure and cardiomyopathy compared to patients who were not treated with chemotherapy [81]. Therefore, cardiac monitoring of women undergoing treatment for breast cancer is of extreme importance, as cardiovascular disease is now the leading cause of death in these survivors, accounting for 15.9% of deaths in one study [82].

Transthoracic echocardiography (TTE) is the first line imaging modality to screen and monitor cardiac function in breast cancer patients undergoing anti-cancer treatment [83]. However, CMR plays a growing role in this field [84]. Current guidelines offer recommendation for administration of potentially cardio-toxic chemotherapy based on LVEF assessment, with a decrease in the LVEF of as little as 10% prompting consideration of withholding therapy in some cases [85]. Therefore, the precise LVEF assessment provided by CMR is of utmost importance in cancer patients in need of cardiotoxic chemotherapy. In addition, a study of patients exposed to anthracyclines has demonstrated that, compared with CMR, 2D echo and 3D TTE had a false-negative rate of 75 and 47%, respectively, for detection of LVEF less than 50% [86]. Finally, TTE examination is often not well tolerated in post-surgical breast cancer patients due to significant discomfort at the post-surgical site. The use of

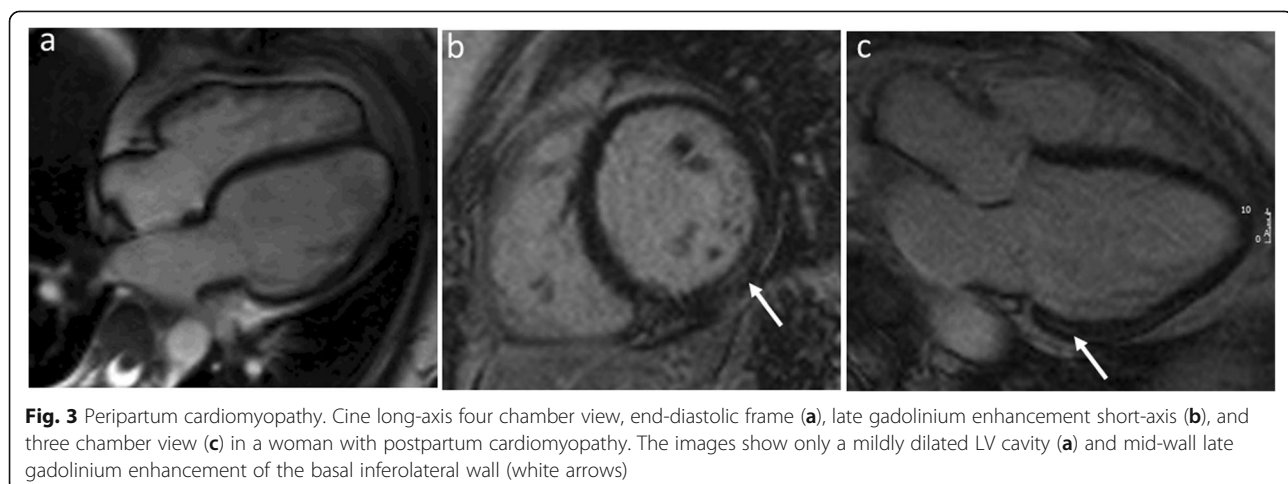


Fig. 3 Peripartum cardiomyopathy. Cine long-axis four chamber view, end-diastolic frame (a), late gadolinium enhancement short-axis (b), and three chamber view (c) in a woman with postpartum cardiomyopathy. The images show only a mildly dilated LV cavity (a) and mid-wall late gadolinium enhancement of the basal inferolateral wall (white arrows)

CMR for assessment of LVEF is indicated to confirm an abnormal LVEF measured by TTE, when TTE images are non-diagnostic, or when the patient cannot tolerate a TTE [87].

Myocardial tissue characterization by CMR guides decision-making on further cardiotoxic therapeutic strategies. CMR can identify preexisting unrecognized myocardial infarctions as well as non-ischemic scar patterns, such as the sub-epicardial linear LGE pattern seen in patients with trastuzumab cardio-toxicity [88]. In some circumstances, stress perfusion CMR may aid in excluding underlying ischemia as the etiology of the cardiomyopathic process [89].

Further advanced cardiac imaging to detect early cardiac dysfunction in women receiving breast cancer therapy is on the horizon. Myocardial strain measured by CMR is clinically feasible [90] and holds promise for monitoring of cardio-toxicity, as determined in one study where strain decreased after low to moderate anthracycline-based therapy ($-17.7 \pm 0.4\%$ to $-15.1 \pm 0.4\%$; $p = 0.0003$) [91]. Other reports [92, 93] suggest that CMR can detect a reduction of LV mass early after anthracycline-based chemotherapy, which was associated with worsening heart failure symptoms, independently of LVEF.

Novel CMR tools such as ECV and native T1 mapping can detect abnormality in the myocardial interstitial spaces after anthracycline exposure as compared to pretreatment values and cancer-free controls (ECV: $30.4 \pm 0.7\%$ vs $27.8 \pm 0.7\%$ and $26.9 \pm 0.2\%$, respectively, $P < 0.01$) [94, 95].

Cardiac involvement in autoimmune and rheumatic disease

Rheumatoid arthritis Rheumatoid arthritis is a multi-system inflammatory disorder affecting 1% of the population, and is 3 times more frequent in women [96]. This condition can be associated with severe cardiovascular

disease that contributes to reduction in life expectancy, especially in patients who are sero-positive for rheumatoid factor [97]. Heart disease in rheumatoid arthritis can present in various forms including: 1) inflammatory reactions of the pericardium, myocardium, and/or endocardium [98] (Fig. 4a), 2) coronary artery disease as ACS, acute MI, or as coronary microvascular dysfunction [99] (Fig. 4b), 3) heart failure due to inflammatory, valvular, or ischemic causes [100], and 4) amyloidosis and restrictive cardiomyopathy [100].

Currently, echocardiography, SPECT, CCT and CMR are used to evaluate the presence and extent of cardiovascular disease in rheumatoid arthritis patients. The advantage of CMR in patients with rheumatoid arthritis is that it is the only currently available non-invasive test that can directly visualize the extent of myocardial involvement in the various forms as mentioned above [101].

Systemic sclerosis Systemic sclerosis is an autoimmune connective tissue disorder that mainly affects women, characterized by vascular dysfunction and multi-organ fibrosis [102, 103]. The heart is commonly involved [102], and the pericardium can also be affected [104]. Direct cardiac involvement may be seen in the form of cardiac fibrosis, myocarditis, dilated cardiomyopathy, heart failure, premature CAD, conduction system abnormalities, and valvular disease. Indirect cardiac involvement can also develop as sequela of pulmonary hypertension (PH) and renal crisis. Cardiovascular disease can remain subclinical, but systemic sclerosis patients with cardiovascular clinical features are at greater risk of deterioration and premature cardiovascular death [105], highlighting the importance of early detection and monitoring of myocardial and vascular involvement in all systemic sclerosis patients [106].

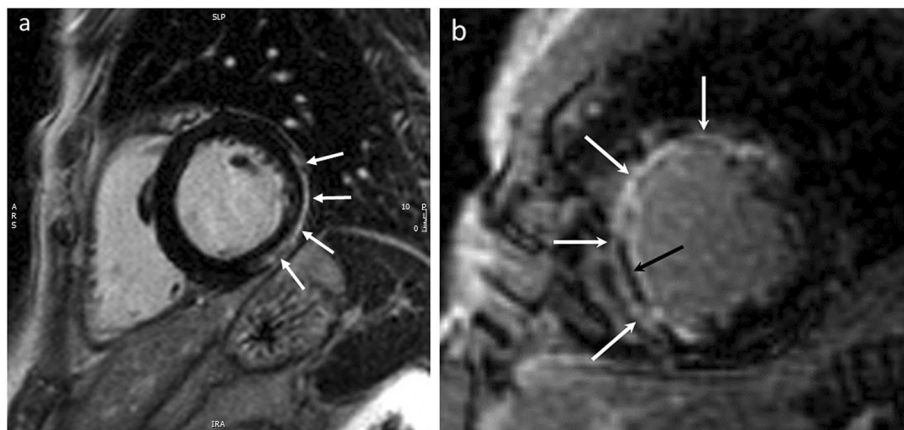


Fig. 4 Rheumatoid arthritis and cardiac injury. Short-axis LGE image in 2 patients with rheumatoid arthritis: the left panel shows epicardial LGE of the basal inferolateral wall (a white arrows), due to myocarditis; the right panel shows near transmural anteroseptal myocardial infarction (b white arrows) with areas of microvascular obstruction (MVO, black arrow), due to left anterior descending coronary artery occlusion

Currently, TTE is the cornerstone investigation for cardiac function, valve morphology, and pulmonary pressure assessment in this population. However, CMR can demonstrate early cardiac abnormalities before cardiac dysfunction. LGE imaging with CMR in systemic sclerosis patients may show evidence of focal fibrosis with a non-ischemic pattern. In the largest CMR study of systemic sclerosis to date, Hachulla et al. found evidence of focal fibrosis in 21% of patients [107]. In the same cohort, CMR detected findings suggestive of myocardial edema in 12% of patients presenting with high signal intensity ratio on T2-weighted imaging [107]. Other authors have reported even higher prevalence of focal LGE in systemic sclerosis patients approaching 43 to 66% [102, 108–110]. In systemic sclerosis patients with LGE (fibrosis or infarction), LV and RV strain have been found to be impaired (–18 to –17% for LV and –22% for RV) compared to systemic sclerosis patients without LGE (–20% for LV and –27% for RV) [111], highlighting the potential role of CMR for detection of early cardiac dysfunction. In systemic sclerosis patients with preserved global ventricular function, Thuny et al. demonstrated impairment in peak LV systolic circumferential strain and peak LV diastolic strain rate by CMR [102].

Other advanced CMR techniques can also detect abnormal myocardial tissue characteristics in systemic sclerosis, including T1 mapping and ECV quantification. Ntusi et al. demonstrated significantly higher native myocardial T1 values in systemic sclerosis patients compared to controls [102]. The same investigators were able to detect a larger area of abnormal myocardial native T1 values (>990 ms) and expansion of ECV beyond the boundaries of myocardial edema on T2-weighted imaging of systemic sclerosis patients, suggesting a combination of low-grade inflammation and increased interstitial volume [102]. The abnormal native T1 and ECV values were associated with worse disease activity and severity [102].

In addition to abnormalities in myocardial tissue characteristics, evidence of microvascular dysfunction has been demonstrated with adenosine stress perfusion CMR in systemic sclerosis patients, with the identification of mostly non-segmental perfusion defects. Kobayashi et al. reported 56% of patients with systemic sclerosis had stress perfusion defects that did not necessarily match the focal fibrosis on LGE [112]. In another study, all systemic sclerosis patients had non-segmental perfusion defects, which were most commonly seen in those with Raynaud's phenomenon and digital ulceration [113]. Finally, perfusion defects in asymptomatic systemic sclerosis patients have also been found to correlate with impaired strain [114].

Systemic lupus erythematosus Systemic lupus erythematosus (SLE) is a chronic, relapsing and remitting,

multisystem inflammatory disorder, occurring 8 to 15 times more commonly in women [115]. Cardiovascular disease is relatively common in SLE, up to 9 times compared to healthy members of the population [116], and many patients have subclinical cardiovascular involvement [117]. Pericarditis, myocarditis, and valve involvement are frequently seen, but most of the excess mortality is due to accelerated atherosclerosis and CAD [116, 118, 119] and lupus coronary arteritis can occur [120]. The rate ratio for MI in women with SLE aged 35 to 44 years is 52 times that of a comparative healthy population in the Framingham cohort [121]. SLE is characterized by several vascular processes, namely inflammation, Raynaud's phenomenon, and a propensity to vascular thrombosis associated with antiphospholipid antibodies, typically in the absence of traditional cardiovascular risk factors [122].

Advanced CMR methods can detect silent myocardial involvement in SLE [123], offering the potential to improve risk stratification and monitor disease progression beyond or in supplement to assessment by echocardiography. Stress perfusion CMR has demonstrated evidence of inducible myocardial ischemia in 44% of subjects with SLE in the absence of obstructive CAD [124]. Myocardial necrosis and fibrosis have been demonstrated by CMR in SLE, with both ischemic and non-ischemic patterns of injury [125–127]. Evidence of active myocarditis has been demonstrated in SLE using T2-weighted imaging [128]. Additional recent evidence suggests that patients with SLE exhibit an increased native T1 and ECV and impaired strain [125], the latter associated with increased arterial stiffness. Finally, impaired myocardial energetics in lupus and rheumatoid arthritis on phosphorous CMR spectroscopy correlated with presence of LGE, myocardial perfusion abnormalities, LA size, ECV and native T1 [129]. Coronary vessel wall imaging by contrast enhanced CMR can detect subclinical enhancement of the coronary vessel wall, a potential novel direct marker of vessel wall injury and remodeling in patients with lupus coronary arteritis [130].

Vasculitis Primary vasculitis is more prevalent in the female population and may be associated with episodic myocardial inflammation, accelerated atherosclerosis, and premature CAD [131]. CMR angiography (CMRA) provides a broad overview of the potential vascular abnormalities in these diseases, including detection and morphologic characterization of aneurysms, aortic valve involvement, coronaries, and branch vessels (subclavian, renal, iliac). CMR can readily detect additional abnormalities of great importance in large vessel vasculitis like Takayasu arteritis, including thrombus, dissection, stenosis of aorta and proximal vessels, vascular inflammation, and pericardial effusions [132]. In addition,

inflammatory, stenotic, or occlusive lesions in the aorta, pulmonary arteries, subclavian, or other peripheral arteries detected by CMRA have been shown to correlate with disease activity [133].

Myocardial injury can be demonstrated using CMR in patients with vasculitis that preferentially involve the heart such as Churg-Strauss syndrome. In a small series of patients with this syndrome and a normal TTE, CMR showed impairment of LV function in about half of the patients, myocardial edema by T2 imaging in a third, and LGE in more than 80% [134]. A pattern of subendocardial LGE has been described in these patients [135].

Duchenne and Becker muscular dystrophies

Duchenne and Becker muscular dystrophies result from mutations in the gene encoding for dystrophin. Female carriers of this X-linked recessive disorder also carry a risk of random X-inactivation that may leave cardiomyocytes with only the abnormal copy, fostering the understanding that these patients may also develop cardiomyopathy [136]. CMR demonstrates a high prevalence of myocardial disease in these patients with nearly half of serially screened female carriers showing either LV dysfunction (14%) or LGE abnormality (44%) in a recent series [137]. The lateral wall epicardial damage identified by LGE mirrors that seen in affected men (Fig. 5), underscoring the genetic mechanism of myocardial disease in these women. Given the high sensitivity of CMR in detecting often subclinical cardiac involvement in female carriers of dystrophin mutations, CMR studies that evaluate the long-term utility of initiating cardioprotective therapy in females are needed, as this is now considered standard of care for men with dystrophinopathies [138].

Women carriers of rare diseases

Fabry Disease is an X-linked lysosomal storage disorder caused by deficiency of the enzyme alpha-galactosidase A, and female carriers have significant cardiac involvement [139, 140]. In the United States, there is an estimated prevalence of 1 in 40,000 to 60,000 males affected by Fabry Disease according to the National Institutes of Health (<https://www.fabrydisease.org>, <https://www.fabry-disease.org/index.php/about-fabry-disease/how-many-people-have-fabry-disease>), but the number of affected female carriers is less understood.

Irrespective of sex, CMR can identify a pre-hypertrophic phenotype in Fabry Disease consisting of both sphingolipid deposits within the myocardium (detect by T1 mapping) and cardiac functional changes [141]. CMR is ideally suited to detect intramyocardial sphingolipid deposits with T1 mapping [142]; LGE and morphological abnormalities are also readily demonstrated.

Global longitudinal strain in Fabry Disease correlates with increased LV mass and presence of electrocardiogram (ECG) abnormalities [143]. In the LV hypertrophy-negative patients, global longitudinal strain is associated with a reduction in T1 mapping, consistent with sphingolipid deposition [143], which can potentially detect early disease in female carriers.

Pulmonary arterial hypertension

Pulmonary hypertension (PH) is characterized by sustained elevation of pulmonary resistance with high mortality rate due to right heart failure [144]. Pulmonary arterial hypertension (PAH) is a rare disease, with manifest precapillary PH characterized by a resting mean pulmonary artery pressure ≥ 25 mmHg, in the presence of LA pressure ≤ 15 mmHg, and with preserved or reduced cardiac output. Survival rates are 67–73% after 3 years [145–147].

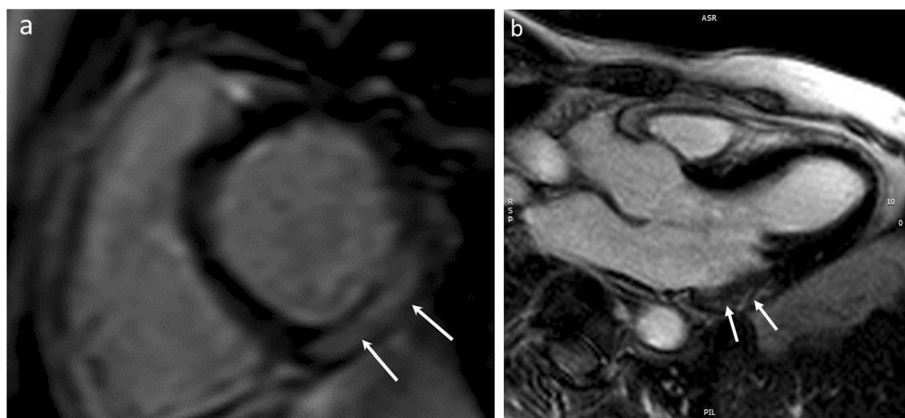


Fig. 5 Duchenne muscular dystrophy. A woman with dystrophin mutation carrier status was screened for myocardial disease with CMR. Late gadolinium enhancement images demonstrated epicardial enhancement of the basal lateral wall in both the short-axis (a) and long-axis views (white arrows), a typical subtle pattern of myocardial injury seen in Duchenne muscular dystrophy

PAH is more common in women, with a particularly high female predominance in patients with PAH secondary to systemic sclerosis, where women constitute more than 80% of the population [144, 148]. CMR studies have shown that women with PAH have better RV function than men at baseline [149], and show greater improvement in RVEF following initiation of PAH-targeted medical treatment [150] compared to men (Fig. 6).

CMR is a reliable method to evaluate cardiac structure and function in PAH patients (Fig. 7), and can be used to predict prognosis [151, 152]. CMR-derived estimation of mean pulmonary arterial pressure has been suggested using septal angle and ventricular mass [153]. Early and reliable detection of ventricular dysfunction is important in patients with PH, and CMR has unique capabilities to quantify RV dysfunction and ventricular septal abnormalities [154]. Fibrosis at the RV insertions on the interventricular septum has been shown by LGE CMR technique in PH [155]. Of note, presence of LGE is related to the degree of RV dysfunction, severity of PH [155, 156], and poorer clinical outcomes [152] in these patients. RA volume measured by CMR can also predict clinical outcomes in PH patients. After multivariate adjustment for RVEF, increased RA volume was still associated with worse clinical outcome in a study of patients with pre-capillary PH, with a lung-transplantation or death hazard ratio of 2.1 (95%CI: 1.1–4.0) [157].

Several CMR biomarkers have been shown to predict mortality in idiopathic PAH, such as RV dilation, smaller RV stroke volume, low RVEF, and impaired LV filling [151]. Deterioration in these variables at follow up are the strongest predictors of poor outcome after 1 year

[151]. The EURO-MR Study suggested that CMR could be used to assess clinical benefit of PAH-targeted medical therapy, where improvement of RV and LV function and volumes was associated with patient survival [158].

Turner syndrome

Turner Syndrome is a genetic disorder affecting 1 in 2500 live female births, characterized by short stature, gonadal dysgenesis, as well as renal and cardiovascular anomalies [159]. Cardiovascular anomalies are present in at least 50% of women with Turner Syndrome [160], and there is an approximately 3-fold increase in age-related risk of mortality primarily due to cardiovascular abnormalities and atherosclerosis [161]. Currently, there is lack of a standardized cardiovascular risk assessment in Turner Syndrome. However, early detection of cardiovascular disorders is critical for initiation of appropriate therapies, and CMR has an expanding role in this population [162].

The most common cardiovascular anomalies in Turner Syndrome include bicuspid aortic valve, aortic dilation, coarctation of the aorta, and anomalous pulmonary venous return [163]. Bicuspid aortic valve (Fig. 8) occurs in up to 30% of women with Turner Syndrome, and has been shown to be associated with an accelerated aortopathy in these patients [164].

CMR is an excellent tool to identify and monitor progression of Turner Syndrome abnormalities [164]. Hjerild et al. reported CMR findings in 102 women with Turner Syndrome and found aortic diameter assessed by CMR correlated with age, blood pressure, bicuspid aortic valve, and a history of aortic coarctation [165]. Aortic

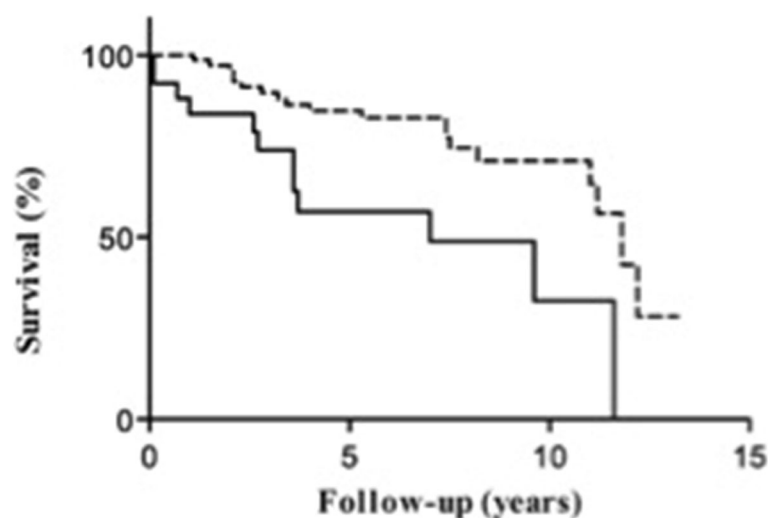


Fig. 6 Sex differences in transplantation-free survival in pulmonary arterial hypertension. Transplant-free survival in male (solid line) and female (dashed line) patients with pulmonary arterial hypertension starting first-line pulmonary arterial hypertension-specific therapies ($P = 0.002$) [150]. Reprinted from CHEST, 145 [5], Jacobs W et al., The Right Ventricle Explains Sex Differences in Survival in Idiopathic Pulmonary Arterial Hypertension, 1230–1236. Copyright (2014), with permission from Elsevier

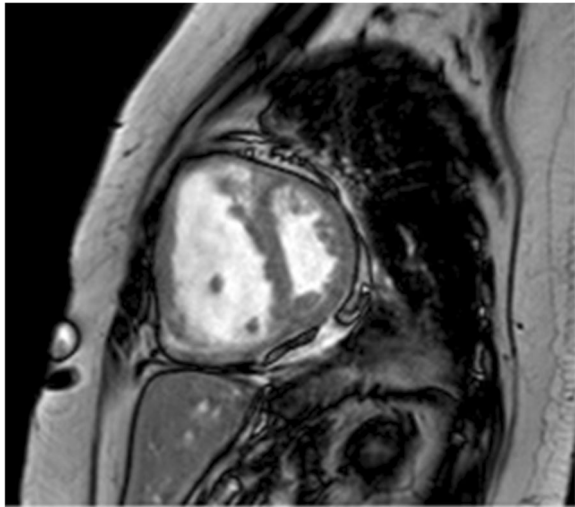


Fig. 7 Pulmonary arterial hypertension. Short axis balanced steady state free precession cine image in patient with precapillary pulmonary hypertension in diastole demonstrating right ventricular dilatation and hypertrophy as well as bulging of the interventricular septum into the small left ventricle as a sign of high pulmonary arterial pressure. The septal flattening can easily be demonstrated by echocardiography, but the biventricular mass, volumetric, and functional quantification using CMR is superior to echocardiographic estimates

dilation is present in 40% of women with Turner Syndrome, and the use of standard absolute values for aortic diameters in these women is inaccurate, owing to their body size. A more appropriate CMR parameter is ascending aortic size indexed to the body surface area, as



Fig. 8 Bicuspid valve. Balanced steady-state, free precession cine CMR in the short-axis plane demonstrating a bicuspid aortic valve in a young woman with Turner syndrome. Echocardiography is first-line modality for assessment of cardiac valves. However, CMR can corroborate the valve morphology in case of suboptimal image quality with echocardiography. RA, right atrium; LA, left atrium; RV, right ventricle

25% of the women with absolute values above 3.5 cm and 33% of the women with indexed values $> 2.5 \text{ cm/m}^2$ are subject to aortic dissection (6- to 100 fold higher) within 3 years of follow-up [166]. Women with Turner Syndrome have an increased risk of aortic dissection, and dissection occurs at a much earlier age than in the general population (30.4 years vs. 77 years) [167, 168]. In addition to assessment of aortic abnormalities, CMR can confirm the presence of anomalous pulmonary venous drainage, which is found in 10–15% of Turner Syndrome cases and can be particularly challenging to diagnosis in adults by TTE [169].

Cardiovascular abnormalities in Turner Syndrome patients may be under-diagnosed in childhood in the absence of screening, as shown in a study of 150 women with Turner Syndrome, where more than 40% of the subjects were found to have unknown cardiac anomalies [170]. As a result, CMR is recommended for screening in all children with Turner Syndrome, regardless of whether any cardiac anomalies have been detected by TTE; however, optimal timing of imaging is unclear. In general, it is recommended that CMR be performed at an age when sedation is not needed [171].

CMR in pregnancy

CMR is a well-established method for imaging cardiovascular disease in pregnant women with potentially life-threatening abnormalities that cannot be completely characterized by TTE [172, 173]. As such, CMR can identify and characterize the severity of cardiovascular conditions that impose a significant risk for mother and offspring, and for which pregnancy is not recommended. Such conditions include Marfan Syndrome with significantly dilated aortic root, complex congenital heart disease (CHD), as well as severe left heart obstructive lesions and LV dysfunction [174]. The main role of CMR in pregnancy is risk stratification to inform the most suitable mode of delivery, to plan adequate cardiovascular care during delivery and postpartum, and to assist in recommendation for pregnancy interruption only when indicated.

The most common indications for CMR during pregnancy are suspected aortic dissection, aortic aneurysm, aortic coarctation, cardiomyopathy/myocarditis, and postoperative complex CHD. While aortic dissection is a rare event during pregnancy, it is associated with up to 10% mortality rate [175]. If dissection occurs, it is most frequently during the third trimester or the postpartum period. Patients with bicuspid aortic valve, aortic coarctation, and collagen vascular diseases have increased risk of aortic dissection [176]. Therefore, it has been suggested that a dilated aorta with a maximum diameter of $> 50 \text{ mm}$ (Fig. 9) in bicuspid aortic valve patients, and $> 45 \text{ mm}$ in Marfan Syndrome patients, is a threshold for



Fig. 9 Dilated ascending aorta in pregnant patient. 3D volume rendering reformation of a non-contrast CMR angiogram in a patient with bicuspid aortic valve and Marfan Syndrome shows dilatation of the ascending aorta (arrow). In this patient with a maximum ascending aortic dimension of 45 mm, close clinical monitoring was recommended during pregnancy and delivery

potential pregnancy interruption during the first trimester [176]. Any woman with Marfan Syndrome presenting with chest or intrascapular pain during pregnancy should have urgent cross-sectional imaging of the aorta to exclude dissection, and this should preferably be with CMR [174].

In pregnant women with postoperative CHD, CMR evaluation should be optimized for quantification of ventricular volumes and function, functionality of conduits, baffles and grafts, as well as assessment of the pulmonary and aortic valves [174, 176]. Of note, high maternal and fetal mortality rates occur with a LVEF < 40%, dilated and dysfunctional systemic RV, as well as pulmonary or aortic valve obstructive lesions [177, 178]. Women with a systemic RV are at particular risk of maternal pregnancy related complications, and a recent analysis of 17 women with transposition of the great arteries who had undergone atrial switch surgery revealed that all pregnancy related cardiac complications occurred in women with a systemic RVEF < 35% [179].

Many women with CHD undergo serial imaging by CMR for cardiovascular surveillance and risk stratification prior or after pregnancy [180, 181]. CMR may be particularly useful in women with moderate or severe forms of CHD for risk stratification. In 28 women with aortic coarctation (4 native, 24 repaired) who underwent CMR within 2 years of pregnancy, a minimum aortic diameter ≤ 12 mm was identified as an important

anatomic determinant of adverse cardiovascular outcomes. For each decrease in absolute aortic diameter of 1 mm, or indexed aortic diameter of 1 mm/m^2 , there was a three-fold increase in odds of occurrence of a cardiovascular event during pregnancy [180]. CMR has also been used to determine the degree of RV remodeling following pregnancy in women with repaired tetralogy of Fallot (TOF). Egidy-Assenza et al. compared data from sequential CMRs from 13 women with repaired TOF who completed pregnancy and from a matched comparison group of 26 nulliparous women with repaired TOF. The rate of increase of indexed RVEDV in the pregnancy group was higher than the comparison group ($4.1 \pm 1.1 \text{ ml/m}^2/\text{year}$ vs. $1.6 \pm 0.6 \text{ ml/m}^2/\text{year}$, $p = 0.07$) [181].

According to CMR safety guidelines, there are no reports of clinical CMR during pregnancy inducing deleterious effects to mother or fetus [182]. Indeed, a recent large cohort study demonstrated that exposure to MRI during the first trimester of pregnancy compared with non-exposure was not associated with increased risk of harm to the fetus or in early childhood [183]. However, the same study showed that exposure of gadolinium-based contrast agent (GBCA) at any time during pregnancy was associated with an increased risk of a broad set of rheumatological, inflammatory, or infiltrative skin conditions and risk of stillbirth or neonatal death [183]. Accordingly, the American College of Radiology does not recommend GBCA administration during pregnancy based on the absence of sufficient evidence to conclude no risk, unless the benefits significantly outweigh the risks to mother and fetus [182]. GBCA should only be administered for CMR examination after non-contrast techniques have been attempted and failed to answer the clinical question.

Conclusions

CMR is high-spatial/temporal resolution, non-invasive, non-ionizing radiation imaging modality that adds value in the identification and prognostication of cardiovascular diseases in both sexes, with unique advantages in women. CMR is particularly suitable to identify early cardiovascular disease by means of myocardial characterization and cardiac functional assessment without the use of radiation. In women with chest pain, CMR is unique in precisely identifying ischemia in the absence of obstructive coronary lesion and in establishing alternate diagnoses for MINOCA. CMR is also useful in early detection, severity assessment and monitoring of cardiac diseases specific to women, such as peripartum cardiomyopathy, chemotherapy induced cardiomyopathy after breast cancer treatment, PAH, rheumatological conditions affecting the heart, and Takotsubo cardiomyopathy.

Finally, in CHD and pregnancy related issues, CMR also provides added benefits compared to other non-invasive imaging modalities. CMR is an excellent tool to evaluate cardiovascular anatomy, function, and pathology in women with cardiovascular diseases.

Abbreviations

ACS: Acute coronary syndromes; AHA: American Heart Association; CAD: Coronary artery disease; CCT: Cardiac computed tomography; CHD: Congenital heart disease; CMR: Cardiovascular magnetic resonance; CMRA: Cardiovascular magnetic resonance angiography; ECG: Electrocardiogram; EF: Ejection fraction; FFR: Fractional flow reserve; GBCA: Gadolinium based contrast agent; LA: Left atrium/left atrial; LAV: Left atrial volume; LAVI: Left atrial volume index; LGE: Late gadolinium enhancement; LV: Left ventricle/left ventricular; LVEDV: Left ventricular volume; LVEDVI: Left ventricular volume index; LVEF: Left ventricular ejection fraction; LVESV: Left ventricular end-systolic volume; LVESVI: Left ventricular end-systolic volume index; LVM: Left ventricular mass; LVMI: Left ventricular mass index; LVSV: Left ventricular stroke volume; LVSVI: Left ventricular stroke volume index; MI: Myocardial infarction; MINOCA: Myocardial infarction in non-obstructed coronary arteries; MRA: Magnetic resonance angiography; MPR: Myocardial perfusion reserve index; MVO: Microvascular obstruction; NSTEMI: Non ST-elevation myocardial infarction; PPCM: Peripartum cardiomyopathy; PAH: Pulmonary arterial hypertension; PH: Pulmonary hypertension; RA: Right atrium/right atrial; RAV: Right atrial volume; RAVI: Right atrial volume index; RV: Right ventricle/right ventricular; RVEDV: Right ventricular end-diastolic volume; RVEDVI: Right ventricular end-diastolic volume index; RVEF: Right ventricular ejection fraction; RVESV: Right ventricular end-systolic volume; RVESVI: Right ventricular end-systolic volume index; SLE: Systemic lupus erythematosus; SPECT: Single-photon emission computed tomography; STEMI: ST-elevation myocardial infarction; TCM: Takotsubo cardiomyopathy; TOF: Tetralogy of Fallot; TTE: Transthoracic echocardiography

Acknowledgments

CBD is in part supported by the Bristol National Institute of Health Research (NIHR) Biomedical Research Centre (BRC). VMF acknowledges support from the British Heart Foundation (BHF), the Oxford National Institute of Health Research (NIHR) Biomedical Research Centre and the Oxford BHF Centre of Research Excellence. The views expressed in this publication are those of the author(s) and not necessarily those of the NHS, the National Institute for Health Research or the Department of Health and Social Care, United Kingdom. We would like to thank Dr. Bostjan Berlot, Bristol Heart Institute, University of Bristol, United Kingdom for helpful expert assistance with the preparation of most manuscript images (Figs. 1, 2, 3, 4 and 8).

Authors' contributions

CBD, KO conceived the manuscript idea. All authors wrote sections of the manuscript, critically reviewed the manuscript, and have read and approved the final version. All authors provided consent to the publication of this manuscript. EO, CBD finalized the manuscript and subsequent revisions.

Funding

Open access funding provided by Lund University. There is no other funding to disclose related to this manuscript.

Availability of data and materials

Data sharing is not applicable to this article as no datasets were generated or analyzed during the current study.

Ethics approval and consent to participate

Not applicable to this article as no datasets were generated or analyzed during the current study.

Consent for publication

Not applicable to this article as no datasets were generated or analyzed during the current study.

Competing interests

CBD is a consultant for Circle Cardiovascular Imaging (Calgary, Canada).

Author details

¹Bristol Heart Institute, Bristol National Institute of Health Research (NIHR) Biomedical Research Centre, University Hospitals Bristol and University of Bristol, Bristol, UK. ²Department of Clinical Sciences Lund, Clinical Physiology, Skåne University Hospital Lund, Lund University, Getingevägen 5, SE-22185 Lund, Sweden. ³Yale University, New Haven, CT, USA. ⁴Oxford Centre for Clinical Magnetic Resonance Research (OxCMR), Division of Cardiovascular Medicine, British Heart Foundation Centre of Research Excellence, Oxford NIHR Biomedical Research Centre, University of Oxford, Oxford, UK. ⁵University of Texas Medical Branch, Galveston, TX, USA. ⁶University of California San Francisco, San Francisco, CA, USA. ⁷Ohio State University, Columbus, OH, USA. ⁸Georgetown University, Washington DC, USA. ⁹Heart and Lung Centre, New Cross Hospital, Wolverhampton, UK. ¹⁰Onassis Cardiac Surgery Center, Athens, Greece. ¹¹University of Cape Town and Groote Schuur Hospital, Cape Town, South Africa. ¹²Charite Hospital, University of Berlin and HELIOS-Clinics Berlin-Buch, Berlin, Germany. ¹³Boston Children's Hospital, Brigham and Women's Hospital, Boston, USA.

Received: 18 May 2018 Accepted: 1 September 2020

Published online: 28 September 2020

References

1. Melloni C, Berger JS, Wang TY, et al. Representation of women in randomized clinical trials of cardiovascular disease prevention. *Circ Cardiovasc Qual Outcomes*. 2010;3:135–42.
2. Dougherty AH. Gender balance in cardiovascular research: importance to women's health. *Tex Heart Inst J*. 2011;38:148–50.
3. Mavrogeni S, Dimitroulas T, Gabriel S, Sfrikakis PP, Pohost GM, Kitis GD. Why currently used diagnostic techniques for heart failure in rheumatoid arthritis are not enough: the challenge of cardiovascular magnetic resonance imaging. *Rev Cardiovasc Med*. 2014;15:320–31.
4. Petersen SE, Aung N, Sanghvi MM, et al. Reference ranges for cardiac structure and function using cardiovascular magnetic resonance (CMR) in Caucasians from the UK biobank population cohort. *J Cardiovasc Magn Reson*. 2017;19:18.
5. Maceira AM, Prasad SK, Khan M, Pennell DJ. Normalized left ventricular systolic and diastolic function by steady state free precession cardiovascular magnetic resonance. *J Cardiovasc Magn Reson*. 2006;8:417–26.
6. Alfakih K, Plein S, Thiele H, Jones T, Ridgway JP, Sivananthan MU. Normal human left and right ventricular dimensions for MRI as assessed by turbo gradient echo and steady-state free precession imaging sequences. *J Magn Reson Imaging*. 2003;17:323–9.
7. Maceira AM, Prasad SK, Khan M, Pennell DJ. Reference right ventricular systolic and diastolic function normalized to age, gender and body surface area from steady-state free precession cardiovascular magnetic resonance. *Eur Heart J*. 2006;27:2879–88.
8. Maceira AM, Cosin-Sales J, Roughton M, Prasad SK, Pennell DJ. Reference left atrial dimensions and volumes by steady state free precession cardiovascular magnetic resonance. *J Cardiovasc Magn Reson*. 2010;12:65.
9. Maceira AM, Cosin-Sales J, Prasad SK, Pennell DJ. Characterization of left and right atrial function in healthy volunteers by cardiovascular magnetic resonance. *J Cardiovasc Magn Reson*. 2016;18:64.
10. Maceira AM, Cosin-Sales J, Roughton M, Prasad SK, Pennell DJ. Reference right atrial dimensions and volume estimation by steady state free precession cardiovascular magnetic resonance. *J Cardiovasc Magn Reson*. 2013;15:29.
11. Petersen SE, Khanji MY, Plein S, Lancellotti P, Bucciarelli-Ducci C. European Association of Cardiovascular Imaging expert consensus paper: a comprehensive review of cardiovascular magnetic resonance normal values of cardiac chamber size and aortic root in adults and recommendations for grading severity. *Eur Heart J Cardiovasc Imaging*. 2019;20(12):1321–31.
12. Dabir D, Child N, Kalra A, et al. Reference values for healthy human myocardium using a T1 mapping methodology: results from the International T1 Multicenter cardiovascular magnetic resonance study. *J Cardiovasc Magn Reson*. 2014;16:69.
13. Liu CY, Liu YC, Wu C, et al. Evaluation of age-related interstitial myocardial fibrosis with cardiac magnetic resonance contrast-enhanced T1 mapping: MESA (Multi-Ethnic Study of Atherosclerosis). *J Am Coll Cardiol*. 2013;62:1280–7.
14. Piechnik SK, Ferreira VM, Lewandowski AJ, et al. Normal variation of magnetic resonance T1 relaxation times in the human population at 1.5 T using ShMOLLI. *J Cardiovasc Magn Reson*. 2013;15:13.

15. Roy C, Slimani A, de Meester C, et al. Age and sex corrected normal reference values of T1, T2 T2* and ECV in healthy subjects at 3T CMR. *J Cardiovasc Magn Reson*. 2017;19:72.
16. Bonner F, Janzarik N, Jacoby C, et al. Myocardial T2 mapping reveals age- and sex-related differences in volunteers. *J Cardiovasc Magn Reson*. 2015;17:9.
17. von Knobelsdorff-Brenkenhoff F, Prothmann M, Dieringer MA, et al. Myocardial T1 and T2 mapping at 3 T: reference values, influencing factors and implications. *J Cardiovasc Magn Reson*. 2013;15:53.
18. Baessler B, Schaarschmidt F, Stehning C, et al. Reproducibility of three different cardiac T2 -mapping sequences at 1.5T. *J Magn Reson Imaging*. 2016;44:1168–78.
19. Messroghli DR, Moon JC, Ferreira VM, et al. Clinical recommendations for cardiovascular magnetic resonance mapping of T1, T2, T2* and extracellular volume: a consensus statement by the Society for Cardiovascular Magnetic Resonance (SCMR) endorsed by the European Association for Cardiovascular Imaging (EACVI). *J Cardiovasc Magn Reson*. 2017;19:75.
20. Mehta LS, Beckie TM, DeVon HA, et al. Acute myocardial infarction in women: a scientific statement from the American Heart Association. *Circulation*. 2016;133:916–47.
21. Hochman JS, Tamis JE, Thompson TD, et al. Sex, clinical presentation, and outcome in patients with acute coronary syndromes. Global use of strategies to open occluded coronary arteries in acute coronary syndromes IIb investigators. *N Engl J Med*. 1999;341:226–32.
22. Rosengren A, Spetz CL, Koster M, Hammar N, Alfredsson L, Rosen M. Sex differences in survival after myocardial infarction in Sweden; data from the Swedish National Acute Myocardial Infarction Register. *Eur Heart J*. 2001;22:314–22.
23. Gehrie ER, Reynolds HR, Chen AY, et al. Characterization and outcomes of women and men with non-ST-segment elevation myocardial infarction and nonobstructive coronary artery disease: results from the can rapid risk stratification of unstable angina patients suppress adverse outcomes with early implementation of the ACC/AHA guidelines (CRUSADE) quality improvement initiative. *Am Heart J*. 2009;158:688–94.
24. Shaw LJ, Shaw RE, Merz CN, et al. Impact of ethnicity and gender differences on angiographic coronary artery disease prevalence and in-hospital mortality in the American College of Cardiology-National Cardiovascular Data Registry. *Circulation*. 2008;117:1787–801.
25. Anderson RD, Pepine CJ. Gender differences in the treatment for acute myocardial infarction: bias or biology? *Circulation*. 2007;115:823–6.
26. Bairey Merz CN, Shaw LJ, Reis SE, et al. Insights from the NHLBI-sponsored Women's Ischemia Syndrome Evaluation (WISE) study: part II: gender differences in presentation, diagnosis, and outcome with regard to gender-based pathophysiology of atherosclerosis and macrovascular and microvascular coronary disease. *J Am Coll Cardiol*. 2006;47:521–9.
27. Canali E, Masci P, Bogaert J, et al. Impact of gender differences on myocardial salvage and post-ischaemic left ventricular remodelling after primary coronary angioplasty: new insights from cardiovascular magnetic resonance. *Eur Heart J Cardiovasc Imaging*. 2012;13:948–53.
28. Langhans B, Ibrahim T, Hausleiter J, et al. Gender differences in contrast-enhanced magnetic resonance imaging after acute myocardial infarction. *Int J Cardiovasc Imaging*. 2013;29:643–50.
29. Pasupathy S, Air T, Dreyer RP, Tavella R, Beltrame JF. Systematic review of patients presenting with suspected myocardial infarction and nonobstructive coronary arteries. *Circulation*. 2015;131:861–70.
30. Dokainish H, Pillai M, Murphy SA, et al. Prognostic implications of elevated troponin in patients with suspected acute coronary syndrome but no critical epicardial coronary disease: a TACTICS-TIMI-18 substudy. *J Am Coll Cardiol*. 2005;45:19–24.
31. Sheifer SE, Canos MR, Weinfurt KP, et al. Sex differences in coronary artery size assessed by intravascular ultrasound. *Am Heart J*. 2000;139:649–53.
32. Vaccarino V, Krumholz HM, Berkman LF, Horwitz RJ. Sex differences in mortality after myocardial infarction. Is there evidence for an increased risk for women? *Circulation*. 1995;91:1861–71.
33. Marroquin OC, Holubkov R, Edmundowicz D, et al. Heterogeneity of microvascular dysfunction in women with chest pain not attributable to coronary artery disease: implications for clinical practice. *Am Heart J*. 2003;145:628–35.
34. Farb A, Burke AP, Tang AL, et al. Coronary plaque erosion without rupture into a lipid core. A frequent cause of coronary thrombosis in sudden coronary death. *Circulation*. 1996;93:1354–63.
35. Sara JD, Widmer RJ, Matsuzawa Y, Lennon RJ, Lerman LO, Lerman A. Prevalence of coronary microvascular dysfunction among patients with chest pain and nonobstructive coronary artery disease. *JACC Cardiovasc Interv*. 2015;8:1445–53.
36. Ibanez B, James S, Agewall S, et al. 2017 ESC guidelines for the management of acute myocardial infarction in patients presenting with ST-segment elevation: the task force for the management of acute myocardial infarction in patients presenting with ST-segment elevation of the European Society of Cardiology (ESC). *Eur Heart J*. 2018;39(2):119–77.
37. Roffi M, Patrono C, Collet JP, et al. 2015 ESC guidelines for the management of acute coronary syndromes in patients presenting without persistent ST-segment elevation: task force for the management of acute coronary syndromes in patients presenting without persistent ST-segment elevation of the European Society of Cardiology (ESC). *Eur Heart J*. 2016;37:267–315.
38. Pathik B, Raman B, Mohd Amin NH, et al. Troponin-positive chest pain with unobstructed coronary arteries: incremental diagnostic value of cardiovascular magnetic resonance imaging. *Eur Heart J Cardiovasc Imaging*. 2016;17(10):1146–52.
39. Reynolds HR, Srichai MB, Iqbal SN, et al. Mechanisms of myocardial infarction in women without angiographically obstructive coronary artery disease. *Circulation*. 2011;124:1414–25.
40. Mauricio R, Srichai MB, Axel L, Hochman JS, Reynolds HR. Stress cardiac MRI in women with myocardial infarction and nonobstructive coronary artery disease. *Clin Cardiol*. 2016;39(10):596–602.
41. Dastidar AG, Baritussio A, De Garate E, et al. Prognostic role of cardiac MRI and conventional risk factors in myocardial infarction with nonobstructed coronary arteries. *J Am Coll Cardiol*. 2019;12(10):1973–82.
42. Caforio AL, Pankuweit S, Arbustini E, et al. Current state of knowledge on aetiology, diagnosis, management, and therapy of myocarditis: a position statement of the European Society of Cardiology Working Group on Myocardial and Pericardial Diseases. *Eur Heart J*. 2013;34:2636–48 2648a–2648d.
43. Mahrholdt H, Goedecke C, Wagner A, et al. Cardiovascular magnetic resonance assessment of human myocarditis: a comparison to histology and molecular pathology. *Circulation*. 2004;109:1250–8.
44. Friedrich MG, Sechtem U, Schulz-Menger J, et al. Cardiovascular magnetic resonance in myocarditis: a JACC white paper. *J Am Coll Cardiol*. 2009;53:1475–87.
45. Ferreira VM, Piechnik SK, Dall'Armellina E, et al. T1 mapping for the diagnosis of acute myocarditis using CMR: comparison to T2-weighted and late gadolinium enhanced imaging. *J Am Coll Cardiol*. 2013;61:1048–58.
46. Ferreira VM, Piechnik SK, Dall'Armellina E, et al. Native T1-mapping detects the location, extent and patterns of acute myocarditis without the need for gadolinium contrast agents. *J Cardiovasc Magn Reson*. 2014;16:36.
47. Radunski UK, Lund GK, Stehning C, et al. CMR in patients with severe myocarditis: diagnostic value of quantitative tissue markers including extracellular volume imaging. *J Am Coll Cardiol*. 2014;7:667–75.
48. Ferreira VM, Schulz-Menger J, Holmvang G, et al. Cardiovascular magnetic resonance in nonischemic myocardial inflammation: expert recommendations. *J Am Coll Cardiol*. 2018;72:3158–76.
49. Fairweather D, Cooper LT Jr, Blauwet LA. Sex and gender differences in myocarditis and dilated cardiomyopathy. *Curr Probl Cardiol*. 2013;38:7–46.
50. Leurent G, Langella B, Fougerou C, et al. Diagnostic contributions of cardiac magnetic resonance imaging in patients presenting with elevated troponin, acute chest pain syndrome and unobstructed coronary arteries. *Arch Cardiovasc Dis*. 2011;104:161–70.
51. Dastidar AG, Rodrigues JC, Ahmed N, Baritussio A, Bucciarelli-Ducci C. The role of cardiac MRI in patients with troponin-positive chest pain and unobstructed coronary arteries. *Curr Cardiovasc Imaging Rep*. 2015;8:28.
52. Emrich T, Emrich K, Abegunewardene N, et al. Cardiac MR enables diagnosis in 90% of patients with acute chest pain, elevated biomarkers and unobstructed coronary arteries. *Br J Radiol*. 2015;88:20150025.
53. Dastidar AG, Frontera A, Palazzuoli A, Bucciarelli-Ducci C. TakoTsubo cardiomyopathy: unravelling the malignant consequences of a benign disease with cardiac magnetic resonance. *Heart Fail Rev*. 2015;20:415–21.
54. Templin C, Ghadri JR, Diekmann J, et al. Clinical features and outcomes of Takotsubo (stress) cardiomyopathy. *N Engl J Med*. 2015;373:929–38.
55. Eitel I, von Knobelsdorff-Brenkenhoff F, Bernhardt P, et al. Clinical characteristics and cardiovascular magnetic resonance findings in stress (takotsubo) cardiomyopathy. *JAMA*. 2011;306:277–86.
56. Perazzolo Marra M, Zorzi A, Corbetti F, et al. Apicobasal gradient of left ventricular myocardial edema underlies transient T-wave inversion and QT interval prolongation (Wellens' ECG pattern) in Tako-Tsubo cardiomyopathy. *Heart Rhythm*. 2013;10:70–7.

57. Rolf A, Nef HM, Mollmann H, et al. Immunohistological basis of the late gadolinium enhancement phenomenon in tako-tsubo cardiomyopathy. *Eur Heart J*. 2009;30:1635–42.
58. Knuuti J, Wijns W, Saraste A, et al. 2019 ESC guidelines for the diagnosis and management of chronic coronary syndromes. *Eur Heart J*. 2020;41(3):407–77.
59. Baïrey Merz CN. Women and ischemic heart disease paradox and pathophysiology. *J Am Coll Cardiol Img*. 2011;4:74–7.
60. Eitel I, Desch S, de Waha S, et al. Sex differences in myocardial salvage and clinical outcome in patients with acute reperfused ST-elevation myocardial infarction: advances in cardiovascular imaging. *Circ Cardiovasc Imaging*. 2012;5:119–26.
61. Johnson BD, Shaw LJ, Buchthal SD, et al. Prognosis in women with myocardial ischemia in the absence of obstructive coronary disease: results from the National Institutes of Health–National Heart, Lung, and Blood Institute–Sponsored Women’s Ischemia Syndrome Evaluation (WISE). *Circulation*. 2004;109:2993–9.
62. Pepine CJ, Anderson RD, Sharaf BL, et al. Coronary microvascular reactivity to adenosine predicts adverse outcome in women evaluated for suspected ischemia results from the National Heart, Lung and Blood Institute WISE (Women’s Ischemia Syndrome Evaluation) study. *J Am Coll Cardiol*. 2010;55:2825–32.
63. Baldassarre LA, Raman SV, Min JK, et al. Noninvasive imaging to evaluate women with stable ischemic heart disease. *J Am Coll Cardiol Img*. 2016;9:421–35.
64. Shaw JL, Nelson MD, Wei J, et al. Inverse association of MRI-derived native myocardial T1 and perfusion reserve index in women with evidence of ischemia and no obstructive CAD: a pilot study. *Int J Cardiol*. 2018;270:48–53.
65. Coelho-Filho OR, Seabra LF, Mongeon FP, et al. Stress myocardial perfusion imaging by CMR provides strong prognostic value to cardiac events regardless of patient’s sex. *J Am Coll Cardiol Img*. 2011;4:850–61.
66. Schwitler J, Wacker CM, Wilke N, et al. Superior diagnostic performance of perfusion-cardiovascular magnetic resonance versus SPECT to detect coronary artery disease: the secondary endpoints of the multicenter multivendor MR-IMPACT II (Magnetic Resonance Imaging for Myocardial Perfusion Assessment in Coronary Artery Disease Trial). *J Cardiovasc Magn Reson*. 2012;14:61.
67. Nagel E, Greenwood JP, McCann GP, et al. Magnetic resonance perfusion or fractional flow reserve in coronary disease. *N Engl J Med*. 2019;380:2418–28.
68. Greenwood JP, Motwani M, Maredia N, et al. Comparison of cardiovascular magnetic resonance and single-photon emission computed tomography in women with suspected coronary artery disease from the Clinical Evaluation of Magnetic Resonance Imaging in Coronary Heart Disease (CE-MARC) Trial. *Circulation*. 2014;129:1129–38.
69. Raman SV, Donnally MR, McCarthy B. Dobutamine stress cardiac magnetic resonance imaging to detect myocardial ischemia in women. *Prev Cardiol*. 2008;11:135–40.
70. Panting JR, Gatehouse PD, Yang GZ, et al. Abnormal subendocardial perfusion in cardiac syndrome X detected by cardiovascular magnetic resonance imaging. *N Engl J Med*. 2002;346:1948–53.
71. Thomson LE, Wei J, Agarwal M, et al. Cardiac magnetic resonance myocardial perfusion reserve index is reduced in women with coronary microvascular dysfunction. A National Heart, Lung, and Blood Institute-sponsored study from the Women’s Ischemia Syndrome Evaluation. *Circ Cardiovasc Imaging*. 2015;8:e002481.
72. Guaricci AI, Carrabba N, Aquaro GD, et al. Advanced imaging techniques (CT and MR): gender-based diagnostic work-up in ischemic heart disease? *Int J Cardiol*. 2019;286:234–8.
73. Mieres JH, Gulati M, Baïrey Merz N, et al. Role of noninvasive testing in the clinical evaluation of women with suspected ischemic heart disease: a consensus statement from the American Heart Association. *Circulation*. 2014;130:350–79.
74. Hilfiker-Kleiner D, Haghikia A, Nonhoff J, Bauersachs J. Peripartum cardiomyopathy: current management and future perspectives. *Eur Heart J*. 2015;36:1090–7.
75. Tidswell M. Peripartum cardiomyopathy. *Crit Care Clin*. 2004;20:777–88 xi.
76. Sliwa K, Skudicky D, Bergemann A, Candy G, Puren A, Sareli P. Peripartum cardiomyopathy: analysis of clinical outcome, left ventricular function, plasma levels of cytokines and Fas/APO-1. *J Am Coll Cardiol*. 2000;35:701–5.
77. Ducas RA, Elliott JE, Melnyk SF, et al. Cardiovascular magnetic resonance in pregnancy: insights from the cardiac hemodynamic imaging and remodeling in pregnancy (CHIRP) study. *J Cardiovasc Magn Reson*. 2014;16:1.
78. Arora NP, Mohamad T, Mahajan N, et al. Cardiac magnetic resonance imaging in peripartum cardiomyopathy. *Am J Med Sci*. 2014;347:112–7.
79. Mouquet F, Lions C, de Groote P, et al. Characterisation of peripartum cardiomyopathy by cardiac magnetic resonance imaging. *Eur Radiol*. 2008;18:2765–9.
80. Haghikia A, Rontgen P, Vogel-Claussen J, et al. Prognostic implication of right ventricular involvement in peripartum cardiomyopathy: a cardiovascular magnetic resonance study. *ESC Heart Fail*. 2015;2:139–49.
81. Bowles EJ, Wellman R, Feigelson HS, et al. Risk of heart failure in breast cancer patients after anthracycline and trastuzumab treatment: a retrospective cohort study. *J Natl Cancer Inst*. 2012;104:1293–305.
82. Patnaik JL, Byers T, DiGiuseppi C, Dabelea D, Denberg TD. Cardiovascular disease competes with breast cancer as the leading cause of death for older females diagnosed with breast cancer: a retrospective cohort study. *Breast Cancer Res*. 2011;13:R64.
83. Plana JC, Galderisi M, Barac A, et al. Expert consensus for multimodality imaging evaluation of adult patients during and after cancer therapy: a report from the American Society of Echocardiography and the European Association of Cardiovascular Imaging. *Eur Heart J Cardiovasc Imaging*. 2014;15:1063–93.
84. Plana JC, Thavendiranathan P, Bucciarelli-Ducci C, Lancellotti P. Multi-modality imaging in the assessment of cardiovascular toxicity in the cancer patient. *J Am Coll Cardiol Img*. 2018;11:1173–86.
85. Mackey JR, Clemons M, Cote MA, et al. Cardiac management during adjuvant trastuzumab therapy: recommendations of the Canadian Trastuzumab Working Group. *Curr Oncol*. 2008;15:24–35.
86. Armstrong GT, Plana JC, Zhang N, et al. Screening adult survivors of childhood cancer for cardiomyopathy: comparison of echocardiography and cardiac magnetic resonance imaging. *J Clin Oncol*. 2012;30:2876–84.
87. Walker J, Bhullar N, Fallah-Rad N, et al. Role of three-dimensional echocardiography in breast cancer: comparison with two-dimensional echocardiography, multiple-gated acquisition scans, and cardiac magnetic resonance imaging. *J Clin Oncol*. 2010;28:3429–36.
88. Fallah-Rad N, Lytwyn M, Fang T, Kirkpatrick I, Jassal DS. Delayed contrast enhancement cardiac magnetic resonance imaging in trastuzumab induced cardiomyopathy. *J Cardiovasc Magn Reson*. 2008;10:5.
89. Jiji RS, Kramer CM, Salerno M. Non-invasive imaging and monitoring cardiotoxicity of cancer therapeutic drugs. *J Nucl Cardiol*. 2012;19:377–88.
90. Scatteia A, Baritussio A, Bucciarelli-Ducci C. Strain imaging using cardiac magnetic resonance. *Heart Fail Rev*. 2017;22:465–76.
91. Drafts BC, Twomley KM, D’Agostino R Jr, et al. Low to moderate dose anthracycline-based chemotherapy is associated with early noninvasive imaging evidence of subclinical cardiovascular disease. *J Am Coll Cardiol Img*. 2013;6:877–85.
92. Neilan TG, Coelho-Filho OR, Pena-Herrera D, et al. Left ventricular mass in patients with a cardiomyopathy after treatment with anthracyclines. *Am J Cardiol*. 2012;110:1679–86.
93. Jordan JH, Castellino SM, Melendez GC, et al. Left ventricular mass change after anthracycline chemotherapy. *Circ Heart Fail*. 2018;11:e004560.
94. Tham EB, Haykowsky MJ, Chow K, et al. Diffuse myocardial fibrosis by T1-mapping in children with subclinical anthracycline cardiotoxicity: relationship to exercise capacity, cumulative dose and remodeling. *J Cardiovasc Magn Reson*. 2013;15:48.
95. Jordan JH, Vasu S, Morgan TM, et al. Anthracycline-associated T1 mapping characteristics are elevated independent of the presence of cardiovascular comorbidities in cancer survivors. *Circ Cardiovasc Imaging*. 2016;9(8):e004325.
96. Kvien TK, Uhlig T, Odegard S, Heiberg MS. Epidemiological aspects of rheumatoid arthritis: the sex ratio. *Ann N Y Acad Sci*. 2006;1069:212–22.
97. Kitas GD, Gabriel SE. Cardiovascular disease in rheumatoid arthritis: state of the art and future perspectives. *Ann Rheum Dis*. 2011;70:8–14.
98. Mavrogeni S, Spargias K, Markussis V, et al. Myocardial inflammation in autoimmune diseases: investigation by cardiovascular magnetic resonance and endomyocardial biopsy. *Inflamm Allergy Drug Targets*. 2009;8:390–7.
99. Douglas KM, Pace AV, Trehan GJ, et al. Excess recurrent cardiac events in rheumatoid arthritis patients with acute coronary syndrome. *Ann Rheum Dis*. 2006;65:348–53.
100. Davis JM 3rd, Roger VL, Crowson CS, Kremers HM, Therneau TM, Gabriel SE. The presentation and outcome of heart failure in patients with rheumatoid arthritis differs from that in the general population. *Arthritis Rheum*. 2008;58:2603–11.

101. Mavrogeni S, Sfikakis PP, Dimitroulas T, et al. Imaging patterns of cardiovascular involvement in mixed connective tissue disease evaluated by cardiovascular magnetic resonance. *Inflamm Allergy Drug Targets*. 2015;14:111–6.
102. Ntusi NA, Piechnik SK, Francis JM, et al. Subclinical myocardial inflammation and diffuse fibrosis are common in systemic sclerosis—a clinical study using myocardial T1-mapping and extracellular volume quantification. *J Cardiovasc Magn Reson*. 2014;16:21.
103. Mayes MD, Lacey JV Jr, Beebe-Dimmet J, et al. Prevalence, incidence, survival, and disease characteristics of systemic sclerosis in a large US population. *Arthritis Rheum*. 2003;48:2246–55.
104. Champion HC. The heart in scleroderma. *Rheum Dis Clin N Am*. 2008;34:181–90 viii.
105. Clements PJ, Lachenbruch PA, Furst DE, Paulus HE, Sterz MG. Cardiac score. A semiquantitative measure of cardiac involvement that improves prediction of prognosis in systemic sclerosis. *Arthritis Rheum*. 1991;34:1371–80.
106. Lindholm A, Hesselstrand R, Radegran G, Arheden H, Ostenfeld E. Decreased biventricular longitudinal strain in patients with systemic sclerosis is mainly caused by pulmonary hypertension and not by systemic sclerosis per se. *Clin Physiol Funct Imaging*. 2019;39:215–25.
107. Hachulla AL, Launay D, Gaxotte V, et al. Cardiac magnetic resonance imaging in systemic sclerosis: a cross-sectional observational study of 52 patients. *Ann Rheum Dis*. 2009;68:1878–84.
108. Tzelepis GE, Kelekis NL, Plastras SC, et al. Pattern and distribution of myocardial fibrosis in systemic sclerosis: a delayed enhanced magnetic resonance imaging study. *Arthritis Rheum*. 2007;56:3827–36.
109. Di Cesare E, Battisti S, Di Sibio A, et al. Early assessment of sub-clinical cardiac involvement in systemic sclerosis (SSc) using delayed enhancement cardiac magnetic resonance (CE-MRI). *Eur J Radiol*. 2013;82:e268–73.
110. Mavrogeni S, Karabela G, Koutsogeorgopoulou L, et al. Pseudo-infarction pattern in diffuse systemic sclerosis. Evaluation using cardiovascular magnetic resonance. *Int J Cardiol*. 2016;214:465–8.
111. Lindholm A, Hesselstrand R, Radegran G, Arheden H, Ostenfeld E. Decreased biventricular longitudinal strain in patients with systemic sclerosis is mainly caused by pulmonary hypertension and not by systemic sclerosis per se. *Clin Physiol Funct Imaging*. 2019;39(3):215–25. .
112. Kobayashi H, Yokoe I, Hirano M, et al. Cardiac magnetic resonance imaging with pharmacological stress perfusion and delayed enhancement in asymptomatic patients with systemic sclerosis. *J Rheumatol*. 2009;36:106–12.
113. Mavrogeni S, Bratis K, van Wijk K, et al. Myocardial perfusion-fibrosis pattern in systemic sclerosis assessed by cardiac magnetic resonance. *Int J Cardiol*. 2012;159:e56–8.
114. Kobayashi Y, Kobayashi H, Giles JT, et al. Detection of left ventricular regional dysfunction and myocardial abnormalities using complementary cardiac magnetic resonance imaging in patients with systemic sclerosis without cardiac symptoms: a pilot study. *Intern Med*. 2016;55:237–43.
115. Murphy G, Isenberg D. Effect of gender on clinical presentation in systemic lupus erythematosus. *Rheumatology*. 2013;52:2108–15.
116. Urowitz MB, Bookman AA, Koehler BE, Gordon DA, Smythe HA, Ogryzlo MA. The bimodal mortality pattern of systemic lupus erythematosus. *Am J Med*. 1976;60:221–5.
117. Doria A, Iaccarino L, Sarzi-Puttini P, Atzeni F, Turriell M, Petri M. Cardiac involvement in systemic lupus erythematosus. *Lupus*. 2005;14:683–6.
118. Bulkley BH, Roberts WC. The heart in systemic lupus erythematosus and the changes induced in it by corticosteroid therapy. A study of 36 necropsy patients. *Am J Med*. 1975;58:243–64.
119. Bartels CM, Buhr KA, Goldberg JW, et al. Mortality and cardiovascular burden of systemic lupus erythematosus in a US population-based cohort. *J Rheumatol*. 2014;41:680–7.
120. Zardi EM, Afeltra A. Endothelial dysfunction and vascular stiffness in systemic lupus erythematosus: are they early markers of subclinical atherosclerosis? *Autoimmun Rev*. 2010;9:684–6.
121. Manzi S, Meilahn EN, Rairie JE, et al. Age-specific incidence rates of myocardial infarction and angina in women with systemic lupus erythematosus: comparison with the Framingham study. *Am J Epidemiol*. 1997;145:408–15.
122. Richter JG, Sander O, Schneider M, Klein-Weigel P. Diagnostic algorithm for Raynaud's phenomenon and vascular skin lesions in systemic lupus erythematosus. *Lupus*. 2010;19:1087–95.
123. Mavrogeni S, Koutsogeorgopoulou L, Markousis-Mavrogenis G, et al. Cardiovascular magnetic resonance detects silent heart disease missed by echocardiography in systemic lupus erythematosus. *Lupus*. 2018;27:564–71.
124. Ishimori ML, Martin R, Berman DS, et al. Myocardial ischemia in the absence of obstructive coronary artery disease in systemic lupus erythematosus. *J Am Coll Cardiol Img*. 2011;4:27–33.
125. Puntmann VO, D'Cruz D, Smith Z, et al. Native myocardial T1 mapping by cardiovascular magnetic resonance imaging in subclinical cardiomyopathy in patients with systemic lupus erythematosus. *Circ Cardiovasc Imaging*. 2013;6:295–301.
126. Seneviratne MG, Grieve SM, Figtree GA, et al. Prevalence, distribution and clinical correlates of myocardial fibrosis in systemic lupus erythematosus: a cardiac magnetic resonance study. *Lupus*. 2016;25:573–81.
127. Singh JA, Woodard PK, Davila-Roman VG, et al. Cardiac magnetic resonance imaging abnormalities in systemic lupus erythematosus: a preliminary report. *Lupus*. 2005;14:137–44.
128. Abdel-Aty H, Siegle N, Natusch A, et al. Myocardial tissue characterization in systemic lupus erythematosus: value of a comprehensive cardiovascular magnetic resonance approach. *Lupus*. 2008;17:561–7.
129. Ntusi NA, Holloway C, Francis JM, et al. Impaired energetics and normal myocardial lipids in rheumatoid arthritis and systemic lupus erythematosus: a phosphorous and proton magnetic resonance spectroscopy and cardiovascular magnetic resonance study. *J Cardiovasc Magn Reson*. 2015;17:O99.
130. Varma N, Hinojar R, D'Cruz D, et al. Coronary vessel wall contrast enhancement imaging as a potential direct marker of coronary involvement: integration of findings from CAD and SLE patients. *J Am Coll Cardiol Img*. 2014;7:762–70.
131. Cohen Tervaert JW. Cardiovascular disease due to accelerated atherosclerosis in systemic vasculitides. *Best Pract Res Clin Rheumatol*. 2013;27:33–44.
132. Raman SV, Aneja A, Jarjour WN. CMR in inflammatory vasculitis. *J Cardiovasc Magn Reson*. 2012;14:82.
133. Jiang L, Li D, Yan F, Dai X, Li Y, Ma L. Evaluation of Takayasu arteritis activity by delayed contrast-enhanced magnetic resonance imaging. *Int J Cardiol*. 2012;155:262–7.
134. Wassmuth R, Gobel U, Natusch A, et al. Cardiovascular magnetic resonance imaging detects cardiac involvement in Churg-Strauss syndrome. *J Card Fail*. 2008;14:856–60.
135. Petersen SE, Kardos A, Neubauer S. Subendocardial and papillary muscle involvement in a patient with Churg-Strauss syndrome, detected by contrast enhanced cardiovascular magnetic resonance. *Heart*. 2005;91:e9.
136. Verhaert D, Richards K, Rafael-Fortney JA, Raman SV. Cardiac involvement in patients with muscular dystrophies: magnetic resonance imaging phenotype and genotypic considerations. *Circ Cardiovasc Imaging*. 2011;4:67–76.
137. Florian A, Rosch S, Bietenbeck M, et al. Cardiac involvement in female Duchenne and Becker muscular dystrophy carriers in comparison to their first-degree male relatives: a comparative cardiovascular magnetic resonance study. *Eur Heart J Cardiovasc Imaging*. 2016;17:326–33.
138. McNally EM, Kaltman JR, Benson DW, et al. Contemporary cardiac issues in Duchenne muscular dystrophy. Working group of the National Heart, Lung, and Blood Institute in collaboration with Parent Project Muscular Dystrophy. *Circulation*. 2015;131:1590–8.
139. Wang RY, Lelis A, Mirocha J, Wilcox WR. Heterozygous Fabry women are not just carriers, but have a significant burden of disease and impaired quality of life. *Genet Med*. 2007;9:34–45.
140. Wilcox WR, Oliveira JP, Hopkin RJ, et al. Females with Fabry disease frequently have major organ involvement: lessons from the Fabry Registry. *Mol Genet Metab*. 2008;93:112–28.
141. Nordin S, Kozor R, Baig S, et al. Cardiac phenotype of prehypertrophic Fabry disease. *Circ Cardiovasc Imaging*. 2018;11:e007168.
142. Pica S, Sado DM, Maestrini V, et al. Reproducibility of native myocardial T1 mapping in the assessment of Fabry disease and its role in early detection of cardiac involvement by cardiovascular magnetic resonance. *J Cardiovasc Magn Reson*. 2014;16:99.
143. Vijapurapu R, Nordin S, Baig S, et al. Global longitudinal strain, myocardial storage and hypertrophy in Fabry disease. *Heart*. 2019;105(6):470–6. .
144. Galie N, Humbert M, Vachiery JL, et al. 2015 ESC/ERS guidelines for the diagnosis and treatment of pulmonary hypertension: the joint task force for the diagnosis and treatment of pulmonary hypertension of the European Society of Cardiology (ESC) and the European Respiratory Society (ERS); endorsed by: Association for European Paediatric and Congenital Cardiology (AEPC), International Society for Heart and Lung Transplantation (ISHLT). *Eur Heart J*. 2016;37:67–119.
145. Benza RL, Miller DP, Barst RJ, Badesch DB, Frost AE, McGoon MD. An evaluation of long-term survival from time of diagnosis in pulmonary arterial hypertension from the REVEAL Registry. *Chest*. 2012;142:448–56.

146. Humbert M, Sitbon O, Yaici A, et al. Survival in incident and prevalent cohorts of patients with pulmonary arterial hypertension. *Eur Respir J*. 2010; 36:549–55.
147. Korsholm K, Andersen A, Kirkfeldt RE, Hansen KN, Mellemkjaer S, Nielsen-Kudsk JE. Survival in an incident cohort of patients with pulmonary arterial hypertension in Denmark. *Pulm Circ*. 2015;5:364–9.
148. Hachulla E, Gressin V, Guillemin L, et al. Early detection of pulmonary arterial hypertension in systemic sclerosis: a French nationwide prospective multicenter study. *Arthritis Rheum*. 2005;52:3792–800.
149. Kawut SM, Lima JAC, Barr RG, et al. Sex and race differences in right ventricular structure and function: the MESA-right ventricle study. *Circulation*. 2011;123:2542–51.
150. Jacobs W, van de Veerdonk MC, Trip P, et al. The right ventricle explains sex differences in survival in idiopathic pulmonary arterial hypertension. *Chest*. 2014;145:1230–6.
151. van Wolferen SA, Marcus JT, Boonstra A, et al. Prognostic value of right ventricular mass, volume, and function in idiopathic pulmonary arterial hypertension. *Eur Heart J*. 2007;28:1250–7.
152. Freed BH, Gombert-Maitland M, Chandra S, et al. Late gadolinium enhancement cardiovascular magnetic resonance predicts clinical worsening in patients with pulmonary hypertension. *J Cardiovasc Magn Reson*. 2012;14:11.
153. Swift AJ, Rajaram S, Hurdman J, et al. Noninvasive estimation of PA pressure, flow, and resistance with CMR imaging: derivation and prospective validation study from the ASPIRE registry. *J Am Coll Cardiol Img*. 2013;6:1036–47.
154. Ostefeld E, Stephensen SS, Steding-Ehrenborg K, et al. Regional contribution to ventricular stroke volume is affected on the left side, but not on the right in patients with pulmonary hypertension. *Int J Cardiovasc Imaging*. 2016;32:1243–53.
155. Sanz J, Dellegrottaglie S, Kariisa M, et al. Prevalence and correlates of septal delayed contrast enhancement in patients with pulmonary hypertension. *Am J Cardiol*. 2007;100:731–5.
156. Blyth KG, Groenning BA, Martin TN, et al. Contrast enhanced-cardiovascular magnetic resonance imaging in patients with pulmonary hypertension. *Eur Heart J*. 2005;26:1993–9.
157. Bredfeldt A, Radegran G, Hesselstrand R, Arheden H, Ostefeld E. Increased right atrial volume measured with cardiac magnetic resonance is associated with worse clinical outcome in patients with pre-capillary pulmonary hypertension. *ESC Heart Fail*. 2018;5:864–75.
158. Chin KM, Kingman M, de Lemos JA, et al. Changes in right ventricular structure and function assessed using cardiac magnetic resonance imaging in bosentan-treated patients with pulmonary arterial hypertension. *Am J Cardiol*. 2008;101:1669–72.
159. Stochholm K, Juul S, Juel K, Naeraa RW, Gravholt CH. Prevalence, incidence, diagnostic delay, and mortality in Turner syndrome. *J Clin Endocrinol Metab*. 2006;91:3897–902.
160. Ho VB, Bakalov VK, Cooley M, et al. Major vascular anomalies in Turner syndrome: prevalence and magnetic resonance angiographic features. *Circulation*. 2004;110:1694–700.
161. Schoemaker MJ, Swerdlow AJ, Higgins CD, Wright AF, Jacobs PA, United Kingdom Clinical Cytogenetics G. Mortality in women with Turner syndrome in Great Britain: a national cohort study. *J Clin Endocrinol Metab*. 2008;93:4735–42.
162. Gutmark-Little I, Backeljauw PF. Cardiac magnetic resonance imaging in Turner syndrome. *Clin Endocrinol*. 2013;78:646–58.
163. Marin A, Weir-McCall JR, Webb DJ, van Beek EJ, Mirsadraee S. Imaging of cardiovascular risk in patients with Turner's syndrome. *Clin Radiol*. 2015;70:803–14.
164. Mortensen KH, Hjerrild BE, Stochholm K, et al. Dilation of the ascending aorta in Turner syndrome - a prospective cardiovascular magnetic resonance study. *J Cardiovasc Magn Reson*. 2011;13:24.
165. Hjerrild BE, Mortensen KH, Sorensen KE, et al. Thoracic aortopathy in Turner syndrome and the influence of bicuspid aortic valves and blood pressure: a CMR study. *J Cardiovasc Magn Reson*. 2010;12:12.
166. Matura LA, Ho VB, Rosing DR, Bondy CA. Aortic dilatation and dissection in Turner syndrome. *Circulation*. 2007;116:1663–70.
167. Carlson M, Silberbach M. Dissection of the aorta in Turner syndrome: two cases and review of 85 cases in the literature. *J Med Genet*. 2007;44:745–9.
168. Carlson M, Airhart N, Lopez L, Silberbach M. Moderate aortic enlargement and bicuspid aortic valve are associated with aortic dissection in Turner syndrome: report of the international Turner syndrome aortic dissection registry. *Circulation*. 2012;126:2220–6.
169. Kim HK, Gottliebson W, Hor K, et al. Cardiovascular anomalies in Turner syndrome: spectrum, prevalence, and cardiac MRI findings in a pediatric and young adult population. *AJR Am J Roentgenol*. 2011;196:454–60.
170. Freriks K, Timmermans J, Beerendonk CC, et al. Standardized multidisciplinary evaluation yields significant previously undiagnosed morbidity in adult women with Turner syndrome. *J Clin Endocrinol Metab*. 2011;96:E1517–26.
171. Bondy CA, Turner Syndrome Study G. Care of girls and women with Turner syndrome: a guideline of the Turner Syndrome Study Group. *J Clin Endocrinol Metab*. 2007;92:10–25.
172. Hiratzka LF, Bakris GL, Beckman JA, et al. 2010 ACCF/AHA/AATS/ACR/ASA/SCA/SCAI/SIR/STS/SVM guidelines for the diagnosis and management of patients with thoracic aortic disease: a report of the American College of Cardiology Foundation/American Heart Association Task Force on Practice Guidelines, American Association for Thoracic Surgery, American College of Radiology, American Stroke Association, Society of Cardiovascular Anesthesiologists, Society for Cardiovascular Angiography and Interventions, Society of Interventional Radiology, Society of Thoracic Surgeons, and Society for Vascular Medicine. *Circulation*. 2010;121:e266–369.
173. Warnes CA, Williams RG, Bashore TM, et al. ACC/AHA 2008 guidelines for the management of adults with congenital heart disease: executive summary: a report of the American College of Cardiology/American Heart Association Task Force on Practice Guidelines (writing committee to develop guidelines for the management of adults with congenital heart disease). *Circulation*. 2008;118:2395–451.
174. Bowater SE, Thorne SA. Management of pregnancy in women with acquired and congenital heart disease. *Postgrad Med J*. 2010;86:100–5.
175. Groth KA, Stochholm K, Hove H, et al. Aortic events in a nationwide Marfan syndrome cohort. *Clin Res Cardiol*. 2017;106(2):105–12.
176. European Society of G, Association for European Paediatric C, German Society for Gender M, et al. ESC guidelines on the management of cardiovascular diseases during pregnancy: the task force on the management of cardiovascular diseases during pregnancy of the European Society of Cardiology (ESC). *Eur Heart J*. 2011;32:3147–97.
177. Silversides CK, Grewal J, Mason J, et al. Pregnancy outcomes in women with heart disease: the CARPREG II study. *J Am Coll Cardiol*. 2018;71:2419–30.
178. Drenthen W, Pieper PG, Roos-Hesselink JW, et al. Outcome of pregnancy in women with congenital heart disease: a literature review. *J Am Coll Cardiol*. 2007;49:2303–11.
179. Jimenez Juan L, Valente AM, Silversides CK, et al. Cardiac magnetic resonance imaging characteristics and pregnancy outcomes in women with Mustard palliation for complete transposition of the great arteries. *Int J Cardiol Heart Vasc*. 2016;10:54–9.
180. Jimenez-Juan L, Krieger EV, Valente AM, et al. Cardiovascular magnetic resonance imaging predictors of pregnancy outcomes in women with coarctation of the aorta. *Eur Heart J Cardiovasc Imaging*. 2014;15:299–306.
181. Egidy Assenza G, Cassater D, Landzberg M, et al. The effects of pregnancy on right ventricular remodeling in women with repaired tetralogy of Fallot. *Int J Cardiol*. 2013;168:1847–52.
182. Expert Panel on MRS, Kanal E, Barkovich AJ, et al. ACR guidance document on MR safe practices: 2013. *J Magn Reson Imaging*. 2013;37:501–30.
183. Ray JG, Vermeulen MJ, Bharatha A, Montanera WJ, Park AL. Association between MRI exposure during pregnancy and fetal and childhood outcomes. *JAMA*. 2016;316:952–61.

Publisher's Note

Springer Nature remains neutral with regard to jurisdictional claims in published maps and institutional affiliations.